

MODELING of TEMPERATURE CONDITIONS of REINJECTION in GEOTHERMAL RESERVOIR'S

Éva Farkas

MOL Plc, Budapest P.O.Box 43, HUNGARY 1311

Key words: thermal simulator, reinjection, Hungary

ABSTRACT

A thermal simulator is presented that originally was developed to model multiphase fluid flow in hydrocarbon reservoirs. The model has a modular structure. The **grid** module, and the fluid module are highly independent parts of the model. The integrated finite-difference form is used. By changing the fluid module (the multicomponent, multiphase hydrocarbon module) to a one component, steam--water system, the model can be used to simulate geothermal reservoirs. A new numerical solution technique is applied: the pressure and temperature distributions are calculated directly, without iterations from the mass and energy balance equations. No mass and energy balance errors occur.

The model was used to examine the decrease of spring rates of the Transdanubian Hévíz **spa**, where the water supply is coming from different temperature sources of a karstic, faulted reservoir. An other application simulated the pressure and temperature distributions of Szentes geothermal field (40 wells)

INTRODUCTION

Computer simulators of geothermal reservoirs have been used since the seventies. The numerical techniques applied by the geothermal models are very similar to those of the hydrocarbon reservoir simulators as the equations to be solved are essentially the same. There are, however, differences between the above two type of reservoirs (i.e. simulation problems) coming from different features of these two energy sources. It is worth to mention here the great sizes and the uncertain boundary conditions of geothermal reservoirs, and the very complex thermodynamic systems of hydrocarbon reservoirs, especially when applying some enhanced oil technologies. Fractured, faulted host rock can be found in both groups of cases. Though, the effects of faults can be more dominant for geothermal reservoirs.

To simulate hydrocarbon displacement processes, two- and three-phase, multicomponent isothermal reservoir simulators have been used since the mid sixties, while the reliable solution techniques of thermal models (of steam injection and in-situ combustion) have been published since the seventies. In the first two decades of model development, different models were used for different problems (such as one-, two- or three-dimensional flow of black oil or compositional fluid description). Since the early eighties it is a usual way to apply the so called general purpose simulators. The mathematical backgrounds of the models are the nonlinear mass and energy conservation equations, the Darcy's equation to simplify the momentum conservation equation, and the equations describe the behavior of the fluid-rock system. It can be seen in the technical literature that the number of solution techniques is great enough due to the many variables of this complex system. Among others, the numerical solution techniques depend on the selection of the primary variables calculated from the conservation equations. A natural selection of the primary variables is the set of the conserved quantities. The characterization of the multicomponent hydrocarbon fluid systems could be simplified by applying a pseudo gas, and a pseudo oil

component. This simplification, with the empirical properties, (such as the relative permeabilities, the capillary functions depending on phase saturations) have led to the black oil models. Then, the phase saturations are used as primary variables, instead of the overall component densities. The temperature has been typical primary variable of thermal hydrocarbon displacement models, too. These latter variables are not suitable to describe all states of a fluid system. The generally used IMPES (implicit pressure, explicit saturation) method has made it difficult to turn to compositional modeling in the seventies.

The pressure is primary variable of the models. The enthalpy is often used as primary variable of geothermal models. This was applied, e.g. by Faust and Mercer (1976). These two variables are suitable in cases of one- or two water phases, as well. In the last years, thermal models of hydrocarbon recovery were published using energy primary variables instead of the temperature [Brandtferger et al. (1991), Mifflin et al. (1991)], too.

When building a reservoir simulator, an appropriate numerical technique can help to write a versatile, and concise program code, and to separate the functionally different parts of a simulator, such as the fluid characterization, the geometrical parameters of the model, the time-discretization techniques. In this paper a solution technique is presented that is suitable to serve as a basis of a general purpose model. The idea of this model originally was developed to simulate isothermal hydrocarbon displacement (Acs et al. 1985), and later extended for thermal cases (Farkas and Valkó 1993). This thermal model was applied to simulate some geothermal problems.

THE GOVERNING DIFFERENTIAL EQUATIONS

The governing differential equations of the model describe the conservation of the components, and the total internal energy. Let us use the notation r_i for the overall component mass density

$$r_i = \sum_{j=1}^{NP} \phi S_j \rho_j C_{ij} \quad (1)$$

and u_T for the total specific internal energy

$$u_T = \sum_{j=1}^{NP} \phi S_j \rho_j u_j + (1 - \phi) c_r \rho_r u_r \quad (2)$$

In Eq. 1 and Eq. 2 the notations: ϕ is the porosity, S_j is the saturation of phase j , ρ_j is the phase density, C_{ij} is the mass concentration of component i in phase j ($i=1, \dots, NC$), ($j=1, \dots, NP$), and u is the specific internal energy; subscript r denotes rock. Then, the mass and energy conservation equations can be written as:

$$\frac{\partial r_i}{\partial t} = \nabla \cdot \left(\sum_{j=1}^{NP} \rho_j C_{ij} \mathbf{v}_j \right) + q_i, \quad i = 1, 2, \dots, NC \quad (3)$$

$$\frac{\partial u_T}{\partial t} = \nabla \left(\sum_{j=1}^{NP} \rho_j h_j \mathbf{v}_j \right) + \nabla (\lambda \nabla T) + q_h + q_l \quad (4)$$

where \mathbf{v}_j is

$$\mathbf{v}_j = -K \frac{k_j}{\mu_j} (\nabla p_j - \rho_j g \nabla z), \quad j=1, \dots, NP. \quad (5)$$

In Eqs. 3-5 the notations: p is the pressure, q_i is the mass rate of component i , h_j is the specific enthalpy of phase j , λ is the thermal conductivity coefficient, T is the temperature, q_h is the energy source rate, q_l is the energy loss rate, K is the absolute permeability, k is the relative permeability, μ_j is the viscosity, g is the gravitational constant, and z is the depth. An additional equation, the in-situ "volume balance" equation is added to complete the basic balance equations. The original volume balance equation was given for isothermal systems by Acs et al. (1985). Now, this equation is modified to take account the thermal effects, too:

$$V_f(p, U_T, \mathbf{m}) \equiv V_p(p) \quad (6)$$

here subscript f , and p refer to fluid, and pore respectively, U_T is the total internal energy, \mathbf{m} is the component mass vector. The volume balance equation expresses, that the fluid system should fill the pore system during the displacement process.

THE DIFFERENCE EQUATIONS

The integrated form of Eqs. 3 and Eq. 4 are used

$$m_i = \int_V r_i dV \quad \text{and} \quad U_T = \int_{V_p+V_f} u_T dV \quad (7)$$

The difference equations will be written for the changes of the primary variables

$$\Delta p = p^n - p^o, \quad \Delta m_i = m_i^n - m_i^o, \quad \Delta U_T = U_T^n - U_T^o. \quad (8)$$

where, superscripts n , and o denote new and old time level. The mass rates L_i (unit mass/unit time/unit pressure difference), and L_{i0} (unit mass/unit time) are introduced

$$L_{ik} = \left[\frac{AK}{d} \right]_k \sum_{j=1}^{NP} \rho_j C_{ij} \frac{k_j}{\mu_j} \quad \text{and} \quad L_{i0} = \sum_{k=1}^M \left[\frac{AK}{d} \right]_k \sum_{j=1}^{NP} \rho_j C_{ij} \frac{k_j}{\mu_j} (p_k^o - p_0^o + \rho_{j,k0} g (z_k - z_0)) + Q_i \quad (9)$$

L_{ik} is the mass rate of component i flowing through the k -th boundary of the volume element ($k=1, \dots, M$). L_{i0} is the explicitly calculated mass rate of the volume element denoted by subscript 0. Similarly, the enthalpy rates LH_k (unit enthalpy/unit time/unit pressure difference) and LH_0 (unit enthalpy/unit time)

$$LH_k = \left[\frac{AK}{d} \right]_k \sum_{j=1}^{NP} \rho_j h_j \frac{k_j}{\mu_j} \quad \text{and}$$

$$LH_0 = \sum_{k=1}^M \left[\frac{AK}{d} \right]_k \sum_{j=1}^{NP} \rho_j h_j \frac{k_j}{\mu_j} (p_k^o - p_0^o + \rho_{j,k0} g (z_k - z_0)) + \sum_{k=1}^M \left[\frac{AK}{d} \right]_k \lambda_k (T_k^o - T_0^o) + Q_h + Q_l. \quad (10)$$

will be used in the difference equations, too. In Eqs. 9 and Eqs. 10 the upstream mobilities are used. Then, the mass changes can be written as

$$\Delta m_{i,0} = \Delta t \sum_{k=1}^M L_{ik} (\Delta p_k - \Delta p_0) + \Delta t L_{i0}, \quad i = 1, 2, \dots, NC \quad (11)$$

The change of internal energy in a volume element is the following:

$$\Delta U_{T,0} = \Delta t \sum_{k=1}^M LH_k (\Delta p_k - \Delta p_0) + \Delta t LH_0 \quad (12)$$

The second term of the right-hand side of Eq. 12 is the explicitly calculated part of the energy change. The heat conduction and heat loss are considered explicitly. The production term is discussed elsewhere (Farkas--Valkó, 1993).

Now, the pressure equation will be derived from the volume balance equation Eq. 6. The first order Taylor approximation is applied to express the equality of volumes at the new time level.

$$V_f^o + \frac{\partial V_f}{\partial p} \Delta p + \frac{\partial V_f}{\partial U_T} \Delta U_T + \sum_{i=1}^{NC} \frac{\partial V_f}{\partial m_i} \Delta m_i = V_p^o + \frac{\partial V_p}{\partial p} \Delta p \quad (13)$$

We can substitute the difference approximation of the energy change [Eq. 12] into the third term on the left-hand side of Eq. 13, and the difference approximations of mass changes [Eqs. 11] into the last term on the left-hand side of Eq. 13. By changing the order of summation for the components and the neighboring elements, rearranging the equation, and using the notation c_p for the total compressibility

$$c_p = \frac{\partial V_f}{\partial p} - \frac{\partial V_p}{\partial p}, \quad (14)$$

and c_k , c_0 , ch_k , and ch_0 denote the volume rates,

$$c_k = \sum_{i=1}^{NC} \frac{\partial V_f}{\partial m_i} L_{ik}, \quad c_0 = \sum_{i=1}^{NC} \frac{\partial V_f}{\partial m_i} L_{i0}, \quad (15)$$

$$ch_k = \frac{\partial V_f}{\partial U_T} LH_k, \quad ch_0 = \frac{\partial V_f}{\partial U_T} LH_0.$$

the concise form of the pressure equation is

$$\left[c_p - \Delta t \sum_{k=1}^M (c_k + ch_k) \right] \Delta p_0 + \sum_{k=1}^M [\Delta t (c_k + ch_k)] \Delta p_k = - \Delta t (c_0 + ch_0) + V_p^o - V_f^o \quad (16)$$

To show the influence of the thermal effects we compare Eq. 16 with the isothermal pressure equation of Acs et al. (1985), which is the following:

$$\left[c_p - \Delta t \sum_{k=1}^M c_k \right] \Delta p_0 + \sum_{k=1}^M \Delta t c_k \Delta p_k = - \Delta t c_0 + V_p^o - V_f^o \quad (17)$$

Now, it can be observed, that Eq. 16 differs from Eq. 17 in the volume rates. We can see clearly now, how the thermal effects modify the isothermal volume rates.

The governing difference equations are Eqs. 11, Eq. 12 and Eq. 16. This set of equations makes it possible to apply a sequential solution technique for the primary variables, i.e. for the pressure, masses and total internal energy. First the pressure changes are determined implicitly from Eq. 16 written for all the volume elements. Then, the mass changes can be calculated explicitly from Eqs. 11 by volume elements, finally the change of the total internal energy can be derived explicitly from Eq. 12 by volume elements.

After determining the new primary variables, the new temperature T is calculated. The variable T is the function of p , U_T , and m . The inverse of the $T(p, U_T, m)$ function is applied. The change of the internal energy U_T can be written from the change of function $U_T(p, T, m)$, too

$$\Delta U_T = \frac{\partial U_T}{\partial p} \Delta p + \frac{\partial U_T}{\partial T} \Delta T + \sum_{i=1}^N \frac{\partial U_T}{\partial m_i} \Delta m_i \quad (18)$$

We have already determined the changes of the primary variables (Δp , Δm_i , and ΔU_T) in the last timestep, and know the U_T partials (referring to the beginning of the timestep). Therefore, the temperature change can be expressed from Eq. 18. At saturation temperature, ΔT cannot be expressed from Eq. 18, because then, U_T is not differentiable with respect T . At steam saturation temperature, however, the temperature can simply be calculated from the saturation pressure

$$T = T_{sw}(p) \quad (19)$$

PRESSURE AND TEMPERATURE CORRECTIONS

The $V_f^\circ - V_p^\circ$ term in Eq. 16 expresses the volumetric error committed in the earlier timesteps. This error is originated from the explicitly calculated volume derivatives. The volumetric error proved to be an appropriate control of the timesteps. The timesteps are chosen in such a way that the volumetric error be kept under a negligible volume. This volume discrepancy will be corrected in the next timestep by modifying the pressure equation. Consequently, this correction term cannot be applied for incompressible systems, and should be small enough (e.g., 0.05% of the pore volume), otherwise it can dominate the pressure equation. This dominance occurs especially at small timesteps.

Now, a new correction step has been introduced that proved to be very useful in the thermal model presented here. The aim of this step is to get the correct temperature. After determining the new temperature from Eq. 18, we can calculate all the thermodynamic properties at the new time level, including the fluid volume and the total internal energy of the volume element. Because of the first-order approximation errors, however, the total internal energy calculated from the function $U_T(p, T, m)$ may not be equal to the internal energy calculated from the energy balance equation Eq. 12. The temperature correction step helps to get the equality

$$U_T^{Eq.12} = U_T(p, T, m) \quad (20)$$

by appropriately modifying T . The Newton, or other iteration method can be used to find T from the nonlinear Eq. 20. The initial value of T , calculated from Eq. 18, is a very good estimation of the new temperature. In our practice, generally, one iteration step is enough to reduce under 10^{-7} the relative energy error

$$\frac{U_T^{Eq.12} - U_T(p, T, m)}{U_T^{Eq.12}} \quad (21)$$

MAIN STEPS OF THE CALCULATIONS

The calculations of a timestep consist of the following

1. Determination of the mass and enthalpy rates: $L_{i,k}$, L_0 , IH_k , LH_0 for each boundary surface (Eqs. 9-10).
2. Determination of the compressibility c_p and volume rates c_k and ch_k of the pressure equations (Eqs. 14-15).
3. Solution of the system of linear pressure equations (Eq. 16 for all the volume elements).
4. Calculation of the component mass changes (Eqs. 11).

5. Calculation of the total internal energy changes (Eq. 12).
6. Calculation of the new temperature (Eqs. 18, 20).
7. Calculation of all the fluid properties from the new set of primary variables (e.g. Appendix of Farkas-Valkó 1993).

Important features of this method:

- the primary variables of the model can apply to any arbitrary fluid system,
- the grid calculations, and the fluid-rock characterization are totally decoupled from the solution technique of the differential equations,
- all the coefficients of the pressure equation have physical meanings.

The above method calculates only the pressure implicitly, masses and energy are calculated explicitly. A fully implicit version can also be realized. An isothermal extension of this volume balance technique is discussed by Farkas (1993). The implicit energy calculation has not yet been worked out.

APPLICATIONS

The model was applied to simulate geothermal reservoirs. A simulation study examined the cause of temperature decrease of the Transdanubian Héviz spa, where the water supply is coming from different temperature springs of a huge karstic fractured reservoir. In this study, the appropriate handling of faults caused the difficulties, especially under the thermal lake that was formed above the intersection of two faults. Héviz is situated near to the lake Balaton (see Fig. 1). In the eighties, a great amount of water (about 13 millions m^3 /month) had to be produced from the extended Transdanubian karstic reservoir to ensure bauxite mining activity at about 25 km north east from Héviz, at Nyírad. The amount of water produced from the thermal wells at Héviz area was increasing in this period, too. At the end of the seventies the natural water influx to lake Héviz was 450 l/s. At the end of the eighties this rate decreased to about 300 l/s. The purpose of the simulation study was to examine the cause of reduction of the natural water source rates. The simulation study examined only a small (2.2 km x 2.1 km) area of the huge reservoir (Fig. 1). We had detailed pressure and temperature distributions of this area due to the many observation wells, and measurements in Héviz regions. The two permeable layers of the area are separated with an impermeable layer (Fig. 2.). The layers at the north east corner of the simulated area are direct connection with the surface (see Fig. 2). The temperature and pressure distributions (in 1979 and in 1988) can be seen on Fig. 3.-5. A special grid was constructed applying radial elements around the thermal water wells of the area, and to model lake Héviz. Fracture volume elements were applied to calculate water flow through the fractures. The connections of the two permeable layers were assumed to exist mainly through the fracture elements. The water could flow to lake-Héviz-volume-element only through fracture elements of the two main fractures of the area. The areal grid points of both permeable layers (not including the radial, and fracture grid points) are demonstrated in Fig. 1. The fluid model assumed to have two components (water and air) to consider free surface volume elements. The measured pressures were given as boundary conditions of the model. For lake-Héviz-volume-element, the water column pressure (at a depth of 40 m) was prescribed. For the thermal wells, the water production rates were given. To complete the conditions, the average water influxes of free surface elements were assumed too. The parameters of the fracture elements were determined by applying the total water rate of the springs known at 1979, (the maximum error of the simulated water level was 1.5 m, see Fig. 4). When using the matched fault parameters, the water outflow to lake Héviz was simulated an error of 3% by the time of 1988. Then, the water level derivation from the measured values was about one meter (see the thin lines in Fig. 5.). When omitting the production wells, the natural

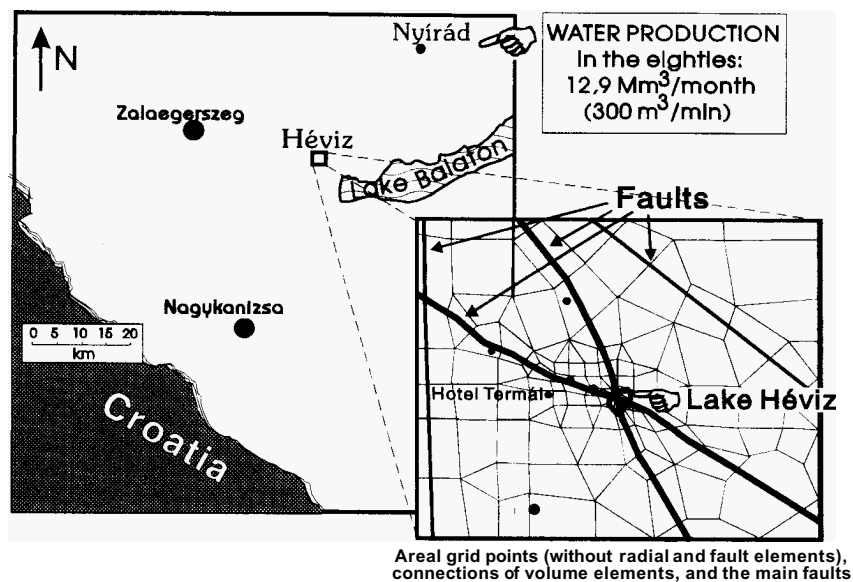


Figure 1. A map of Hévíz surroundings with Nyírad, and the model size

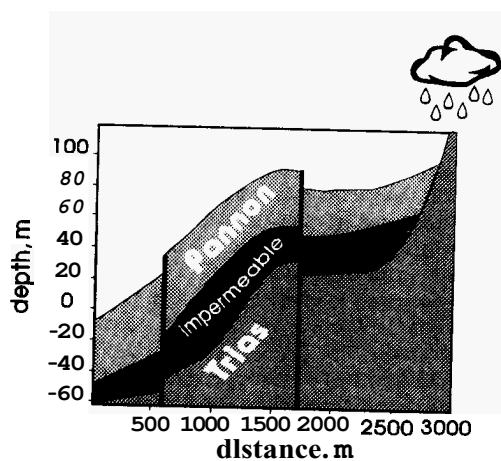


Figure 2. A simplified SW-NE cross section

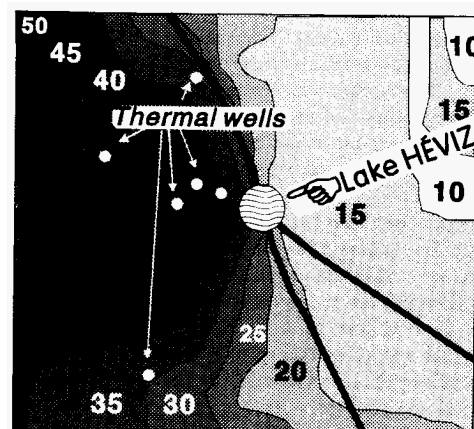


Figure 3. Temperature distribution in Pannon layer, °C

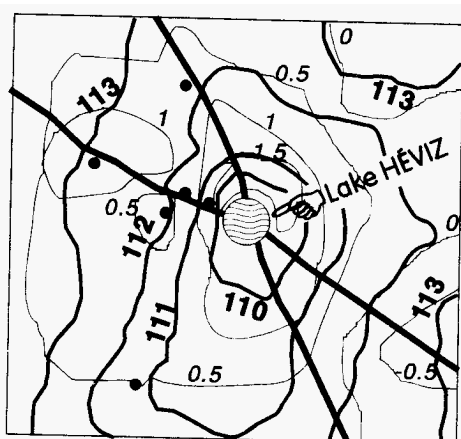


Figure 4. Measured water levels in Pannon layer (m on Balti see level), 1979
the thin lines show the differences of the measured and simulated values

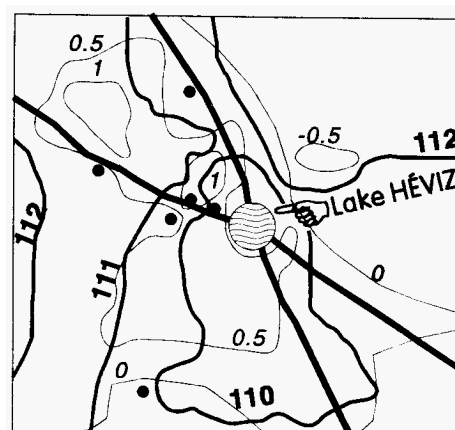


Figure 5. Measured water levels in Pannon layer (m on Balti see level), 1988
the thin lines show the differences of the measured and simulated values

outflow rate to lake Hévíz was increased only by 20% of the total production of thermal wells. The calculated temperature of the water flowing to the lake was 9 °C colder than the measured average of the sources.

The mining activity, i.e. the water production at Nyírád had been stopped at the early eighties because of the environmental damages. Thus, to clear the above questions, and examine other simulation problems no additional support was given. The above work was done in 1989. Since stopping water production at Nyírad, a slow rise of the natural springs' rates in Hévíz can be observed. Now, this rate is over 370 l/s.

In an other application the model was used to simulate the geothermal field of Szentes that is a part of the huge extent Pannon sandstone layers. The first thermal well was drilled in the sixties to heat greenhouses. Belonging to different owners, the number of wells had increased to forty by the end of the eighties, while the average value of the well rates was continuously decreasing from 600,000 m³/year to 300,000 m³/year.

A two dimensional model was used to simulate the history of production including only a part (about 100 km X 100 km area) of the Upper Pannon sandstone reservoir. A problem was to give the appropriate water rates referring to the boundaries of the model to specify the connection between the whole and the model areas. Different boundary conditions were used including the two limits: (1) closed reservoir, (2) unlimited water supply; and to assume the pressure declines at the boundary of the area. Applying the variations of boundary conditions, the simulation runs showed no differences of the average pressure level in near Szentes area for the first five years of production. The pressure level of the geothermal field depended on local production of the individual wells, and the long distance boundary conditions ensuring water supply of the model. The pressure level could partly be regenerated during summer period when production was reduced or stopped, but the water supply rate of the area was less than the produced water rate. The effect of water injection was examined.

The injection wells were simulated about 20 km from the production wells. This distance was far enough to prevent cold water breakthrough, and the pressure decline could be partly reduced.

To examine the behavior of the model in case of two water phases, a steam injection problem (an SPE comparative solution project) was simulated (see Farkas-Valkó 1993).

ACKNOWLEDGEMENT

Many thanks to Tivadar Böcker for the measurements and preparation all reservoir, and production data used in Hévíz model.

REFERENCES

- Ács, G. Doleschall S., and Farkas, É. (1985) General Purpose Compositional Model, SPEJ, Aug. (543-553)
- Brantferger, K.M., Pope, G.A., and Sepehrmoori, K. (1991) Development of a Thermodynamically Consistent, Fully Implicit, Equation of State, Compositional Steamflood Simulator, paper SPE 21253 presented at the Eleventh SPE Symposium on Reservoir Simulation
- Farkas, É. (1993) Adaptive Implicit Volume Balance Techniques, paper SPE 25973, 12th Symposium on Reservoir Simulation, (467-479).
- Farkas, É., Valkó, P. (1993) A Direct IMPES-type Volume Balance Technique for Adaptive Implicit Steam models, paper SPE 26127, SPE Advanced Technology Series, Vol.2, No.2, April 1994 (88-94)
- Faust, C.R. and Mercer, J.W. (1976): An Analysis of Finite-Difference and Finite-Element Techniques for Geothermal Reservoir Simulation, paper SPE 5742 presented at the Fourth SPE Symposium on Reservoir Simulation
- Mifflin, R.T., Watts, J.W., and Weiser, A. (1991): A Fully Coupled, Fully Implicit Reservoir Simulator for Thermal and Other Complex Reservoir Processes, paper SPE 21252 presented at the 11th SPE Symposium on Reservoir Simulation